

RESEARCH PAPER

Photo-degradation of Acid Violet, Acid Blue and Methyl Orange: Photo-catalyst and Magnetic CoFe₂O₄-ZnS Nanocomposite Preparation of Ni, Co, Cu or Ag-doped ZnS Nanoparticles

Mohamad Sabzevari ¹, Sara Azarakhsh ^{1*}, Davood Ghanbari ²

¹ Department of Physics, Faculty of Khorramabad, Lorestan Branch, Technical and Vocational University (TVU), Iran

² Department of Science, Arak University of Technology, Arak, Iran

ARTICLE INFO

Article History:

Received 08 May 2021

Accepted 19 August 2021

Published 01 October 2021

Keywords:

CoFe₂O₄

Nanocomposite

Photo-catalyst

Zinc sulphides

ABSTRACT

In this study CoFe₂O₄ nanostructures were synthesized via a facile precipitation method without using any surfactant and capping agent in solvent of water. Then Zinc sulphides with various doping metals (Ni, Co, Cu and Ag) were prepared. Finally metal doped CoFe₂O₄-ZnS nanocomposites were made by a fast chemical procedure. The prepared products were subjected to various analyses of structural (XRD), optical (UV-visible), the formation of bonds using the (FTIR) spectrometry and surface layer morphology via SEM. Vibrating sample magnetometer shows the ferromagnetic property of the ferrite nanostructures. The photocatalytic behaviour of CoFe₂O₄-ZnS-metal doped nanocomposites was evaluated using the degradation of three azo dyes (acid violet, acid blue, methyl orange) under ultraviolet light irradiation. The results introduce a nanocomposite with applicable magnetic and photocatalytic performance.

How to cite this article

Sabzevari M, Azarakhsh S, Ghanbari D. Photo-degradation of Acid Violet, Acid Blue and Methyl Orange: Photo-catalyst and Magnetic CoFe₂O₄-ZnS Nanocomposite Preparation of Ni, Co, Cu or Ag-doped ZnS Nanoparticles J Nanostruct, 2021; 11(4):744-753. DOI: 10.22052/JNS.2021.04.012

INTRODUCTION

At present, understanding the scientific properties of environmental pollution from different perspectives is economically very valuable. Much research has been done to find a method using photocatalysis to decompose toxic and organic pollutants [1-3]. The use of photocatalyst has attracted attention as an affective way to segregate, remove, and purify several contaminants. Centralized research on heterogeneous photocatalysts have been made to develop photocatalyst technology

* Corresponding Author Email: Sara.azara@yahoo.com

with high performance and low cost for treating pollutants present in toxic wastewater and organic waste with many unique properties [4-6]. Nanosubstances such as ZnO and metal sulfides are known to have excellent photocatalytic activity in the decomposition and purification of various contaminating components [7-10]. Zinc sulfide (ZnS), one of metal sulfides, has thermodynamic optimum conditions for photocatalytic oxidation-reduction reactions. It has been used to produce a highly efficient photocatalyst with an appropriate band potential of electricity. [11-13]. Among these,



This work is licensed under the Creative Commons Attribution 4.0 International License.

To view a copy of this license, visit <http://creativecommons.org/licenses/by/4.0/>.

ZnS (bandgap energy: 3.6–3.8 eV) has served as one of the most efficient photocatalysts for wastewater treatment. It is a very significant transition metal sulfide that can be used in a number of practical application fields such as electrocatalysts and photocatalysts [14–15]. Ferrite nanoparticles have a strong magnetic property, which can be easily used for magnetic separation after degradation. In this work, CoFe₂O₄, a typical ferromagnetic oxide with a spinel structure with a Curie temperature around 793 K [16] is chosen as the magnetic material. Besides its large magnetic anisotropy and moderate saturation magnetization, CoFe₂O₄ has remarkable chemical stability and mechanical hardness. Nanocomposites with properties of photocatalysis, magnetism, based on ZnS and CoFe₂O₄ have been reported. Therefore, the combination of CoFe₂O₄ and ZnS to form core-shell structure nanocomposites will make them have multiple properties. Nanocomposites with ZnS nanoparticles can be fabricated to have a variety of physical, thermal, and other unique properties with many advantages. It has superior properties than existing microscale composite materials. In addition, it can be synthesized using simple and inexpensive technology [17–19]. They have excellent mechanical, chemical, and thermal properties with water resistant function [20–24]. This study describes the synthesis and characterization of nanosized CoFe₂O₄ particles using precipitation method. Investigated the formation of monodispersed nanoparticles in transition metal ion (Ni, Co, Cu, Ag)-doped ZnS. The prepared ion-doped ZnS nanoparticles were compared in the same environment in terms of morphology and structure properties. Finally metal doped CoFe₂O₄-ZnS-Ag nanocomposites were prepared by a fast chemical procedure.

MATERIALS AND METHODS

NiSO₄·6H₂O, Zn(CH₃COO)₂·2H₂O, FeCl₃·6H₂O, Cu(CH₃COO)₂·2H₂O, Co(CH₃COO)₂·4H₂O, AgNO₃, CoSO₄, NaOH, thiourea were purchased from Merck or Aldrich and all the chemicals were used as received without further purifications. A multiwave ultrasonic generator (Bandeline MS 73), equipped with a converter/transducer and titanium oscillator, operating at 20 kHz with a maximum power output of 150 W was used for the ultrasonic irradiation. Room temperature magnetic properties were investigated using an alternating gradient force magnetometer (V)

device made by Meghnatis Kavir Kashan Company (Iran) in an applied magnetic field sweeping between ±10000 Oe. XRD patterns were recorded by a Philips, X-ray diffractometer using Ni-filtered CuK_α radiation. SEM images were obtained using a LEO instrument model 1455VP. Prior to taking images, the samples were coated by a very thin layer of Pt (using a BAL-TEC SCD 005 sputter coater) to make the sample surface conductor and prevent charge accumulation, and obtaining a better contrast.

Synthesis of CoFe₂O₄ nanoparticles

0.2 g of CoSO₄ and 0.4 g of FeCl₃·6H₂O were dissolved in 200 ml of deionized water. Then 45 ml of NaOH solution (1M) was then slowly added to the solution until reaching pH to 10. A brown precipitate was then centrifuged and rinsed with distilled water. Finally obtained precipitate was calcinated at 85°C and its colour goes from brown to black.

Synthesis of ZnS-metal-doped (weight percent: 90%:10%) nanocomposite

0.9 g (90%) of Zn(CH₃COO)₂·2H₂O and 0.1g (10%) of metal doping agents Cu(CH₃COO)₂·2H₂O, Co(CH₃COO)₂·4H₂O, NiSO₄·6H₂O and AgNO₃ were dissolved in 100 ml of deionized water and 30 minutes stirring, then 0.13 g of thiourea dissolved in 100 ml water and it was added to the solution. NaOH solution (1M) was added to the solution (pH:10) and it was stirred for 20 minutes.

Synthesis of CoFe₂O₄-ZnS-metal-doped (100:90:10 %) nanocomposite

0.1 g (100%) of CoFe₂O₄ was dispersed in 100 ml of deionized water by ultrasonic waves for 60 min. Then 0.18 g Yield of ZnS (90%) of Zn(CH₃COO)₂·2H₂O and 0.02g (10%) of metal doping agents AgNO₃, Cu(CH₃COO)₂·2H₂O, (Co(CH₃COO)₂·4H₂O, NiSO₄·6H₂O were dissolved in 100 ml of deionized water and added to the mixture containing CoFe₂O₄. After 30 minutes the mixture of 0.13 g of thiourea (dissolved in 100 ml of deionized water) was transferred into the mixture. NaOH solution was slowly added to the aqueous (pH:10) solution and was stirred for 20 minutes.

Photo-catalytic degradation process

20 ml of the dye solution (10 ppm) was used as a model pollutant to determine the photocatalytic activity. 0.02 g catalyst was applied for degradation

of 20 ml solution. The solution was mixed by a magnet stirrer for 1 hour in darkness to determine the adsorption of the dye by catalyst and better availability of the surface. The solution was irradiated by a 40 W UV lamp which was placed in a quartz pipe in the middle of reactor. It was turned on after 1 hour stirring the solution and sampling (about 10 ml) was done every 20 min [25-30]. The samples were filtered, centrifuged and their concentration was determined by UV-Visible spectrometry.

RESULTS AND DISCUSSION

The Powder XRD measurement was done for the $\text{CoFe}_2\text{O}_4\text{-ZnS-Ag}$ to characterize the phase

and crystallization. Fig. 1 shows the composition of the $\text{CoFe}_2\text{O}_4\text{-ZnS-Ag}$ nanocomposite was also investigated. Presence of both cubic phase was confirmed and are illustrated. The crystalline sizes from Scherrer equation, $D_c = K\lambda/\beta\cos\theta$, was calculated, where β is the width of the observed diffraction peak at its half maximum intensity (FWHM), K is the shape factor, which takes a value of about 0.9, and λ is the X-ray wavelength (CuK_α radiation, equals to 0.154 nm). The average crystalline size for $\text{CoFe}_2\text{O}_4\text{-ZnS-Ag}$ nanoparticles were found to be about 20 respectively. Scanning electron microscopy was employed for estimation of morphology and particle size of the products. SEM image of CoFe_2O_4 nanoparticle are show in Fig.

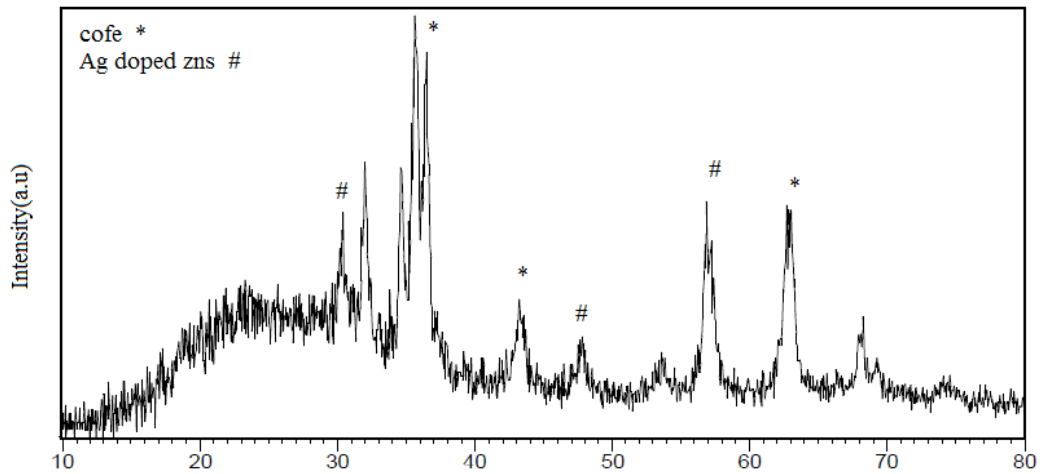


Fig. 1. XRD pattern of $\text{CoFe}_2\text{O}_4\text{-ZnS-Ag}$ -doped nanocomposite

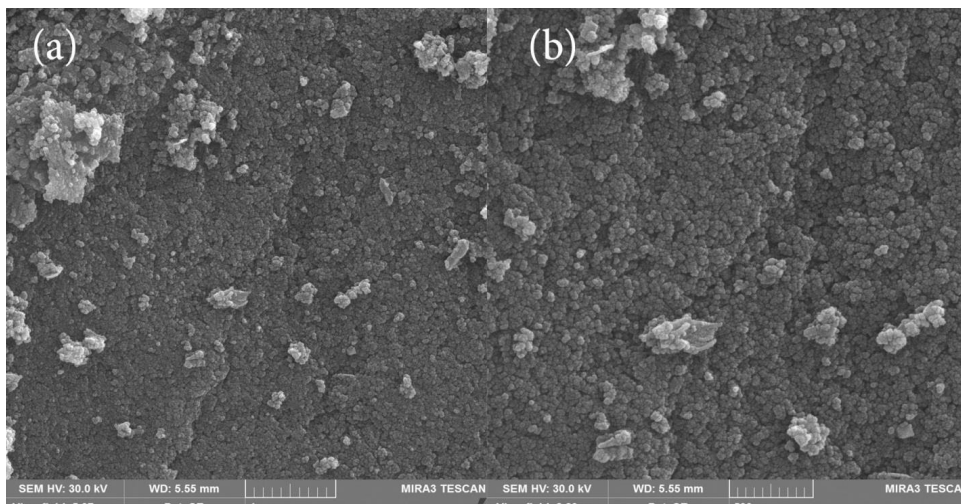


Fig. 2. SEM images of cobalt ferrite nanoparticles

2. surfactant-free CoFe_2O_4 nanoparticles obtained at 85°C in 200 ml of solvent. The particle size and magnetic properties can be easily controlled by changing in precursors. SEM images of the Ag-doped Zinc sulphide nanoparticles are show in Fig. 3. According to scanning electron microscopy images the average particle size is found to be around 59 nm .Figs.4 shows SEM images of the Ni-doped Zinc sulphide nanoparticles. results confirm bigger product was prepared. Fig. 5 illustrate SEM images of the Co-doped cadmium sulphide nanoparticles. SEM images of the Cu-doped cadmium sulphide nanoparticles are shown in Figs.6. Images approve formation of nanoparticles with a little agglomeration. Figs.7 illustrate SEM images of the as-synthesized $\text{CoFe}_2\text{O}_4\text{-ZnS-Ag}$

obtained at 80°C in 200ml of solvent. That result confirms nanocomposites with average size around 29 nm were obtained. The FT-IR spectra of Ag-doped ZnS nanoparticles were obtained at wavelengths ranging from 4000 cm^{-1} to 500 cm^{-1} (Fig. 8). Bands of 664 and 1043 cm^{-1} in sample are characteristic peaks of the Zn-S bond. The spectrum exhibits broad absorption peak around 3414 cm^{-1} , corresponding to the stretching mode of O-H group of hydroxyl group and the band of 1617 cm^{-1} are associated with the functional C=O groups .Fig. 9 shows magnetic property of sample was studied using AGFM instrument and the obtained . Magnetization curve of $\text{CoFe}_2\text{O}_4\text{-ZnS-Ag}$ that also exhibits also ferromagnetic behaviour with a coercivity of about 350 Oe and saturation

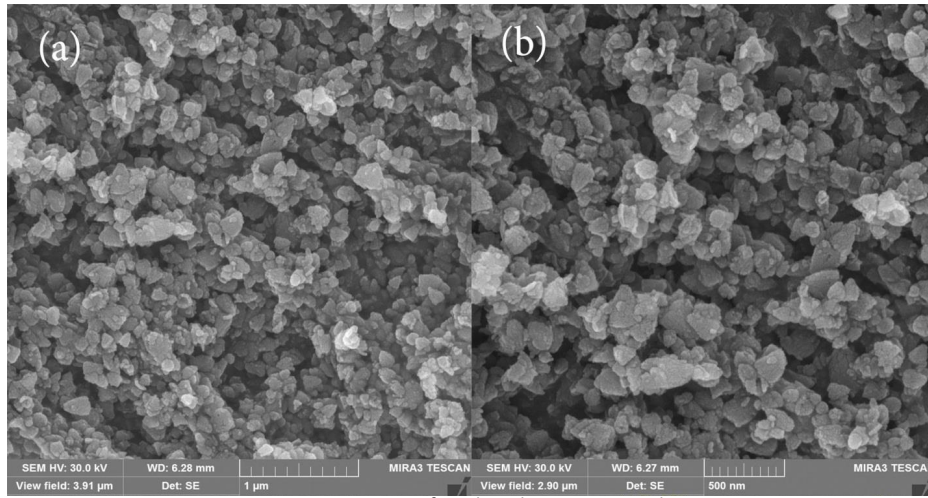


Fig. 3. SEM images of Ag-doped ZnS nanoparticles

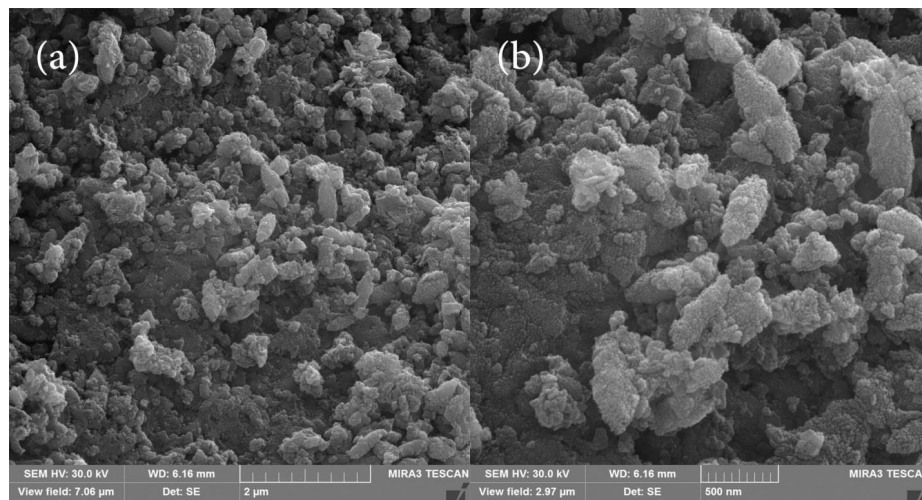


Fig. 4. SEM images of Ni-doped ZnS nanoparticles

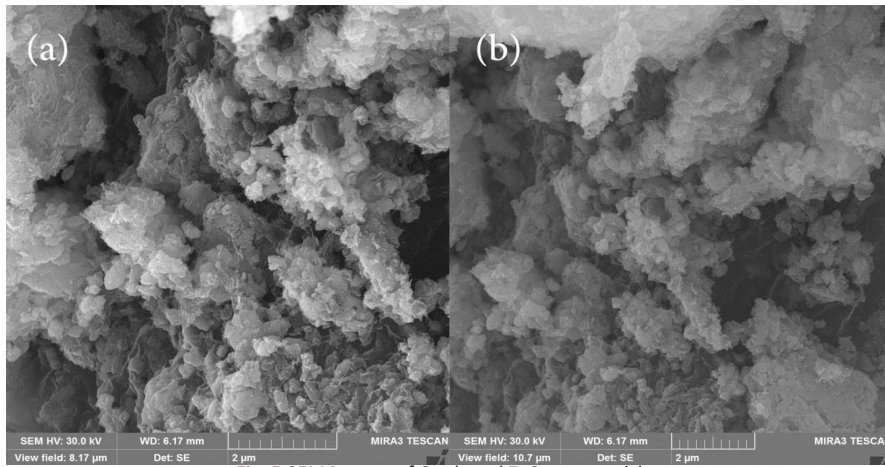


Fig. 5. SEM images of Co-doped ZnS nanoparticles

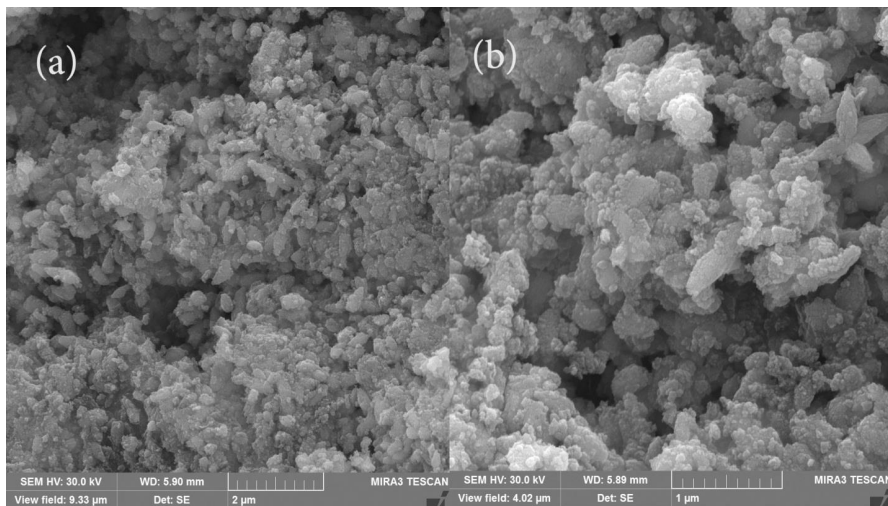


Fig. 6. SEM images of Cu doped ZnS nanoparticles

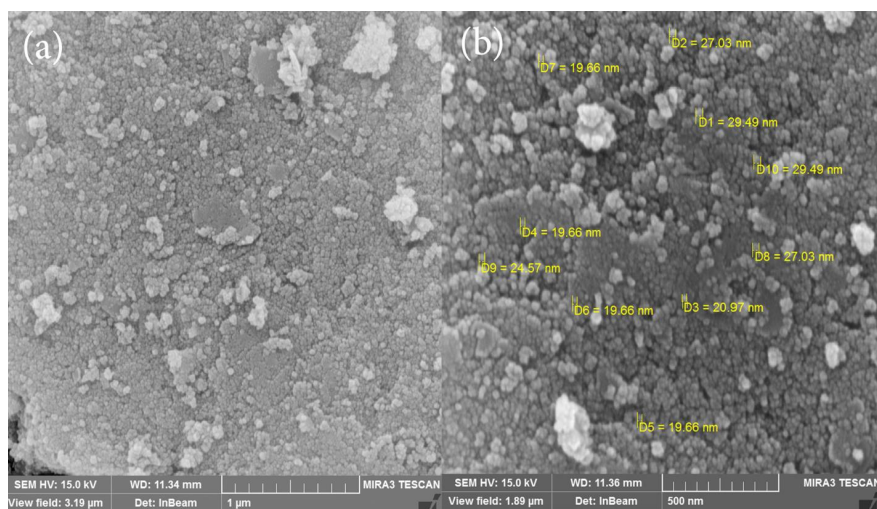


Fig. 7. SEM images of $\text{CoFe}_2\text{O}_4\text{-ZnS-Ag}$ -doped nanocomposite

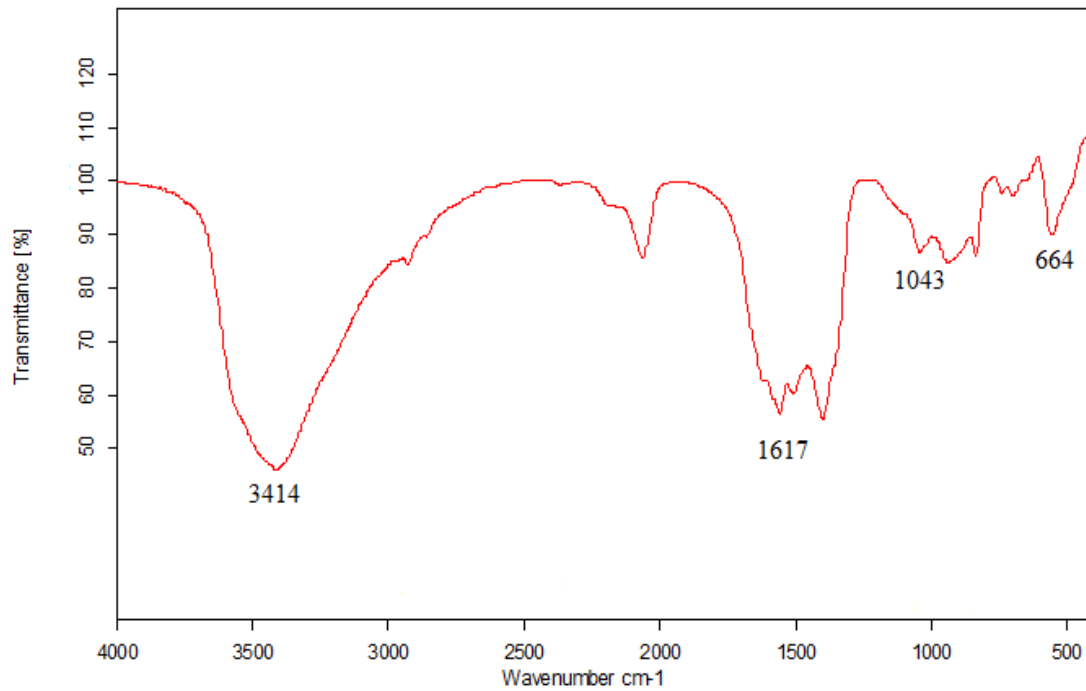


Fig. 8. FT-IR of Ag-doped ZnS nanoparticles

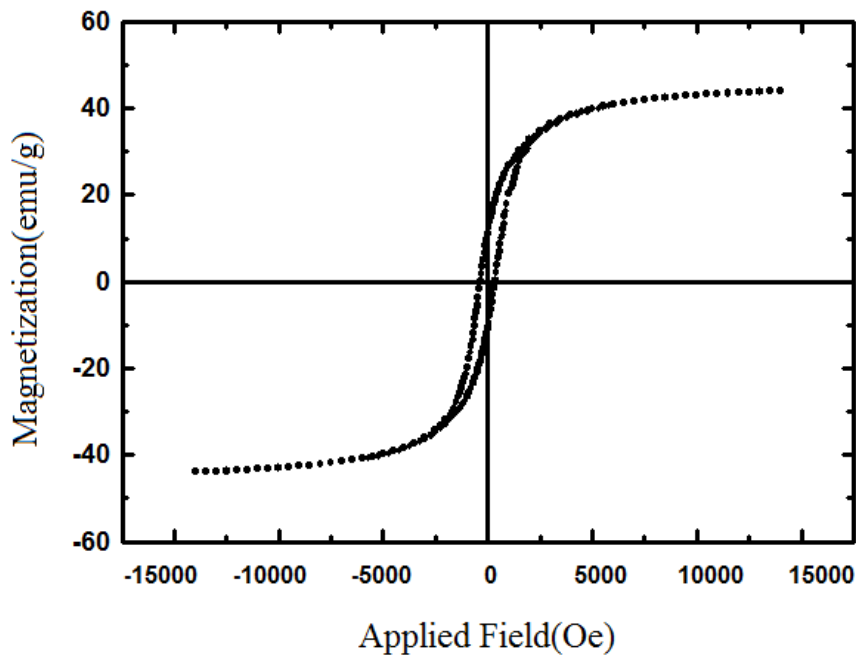


Fig. 9. AGFM curve of $\text{CoFe}_2\text{O}_4\text{-ZnS}$ -Ag-doped nanocomposite

magnetization of 43 emu/g. The magnetic property of the prepared nanocomposites is an essential characteristic of a heterogeneous nanocomposite since materials with this magnetic behaviour have

low tendency in inter-particles agglomeration caused by dipole-dipole interaction in comparison with ferromagnetic nanocomposites. The photo-catalytic activity of the nanocomposite

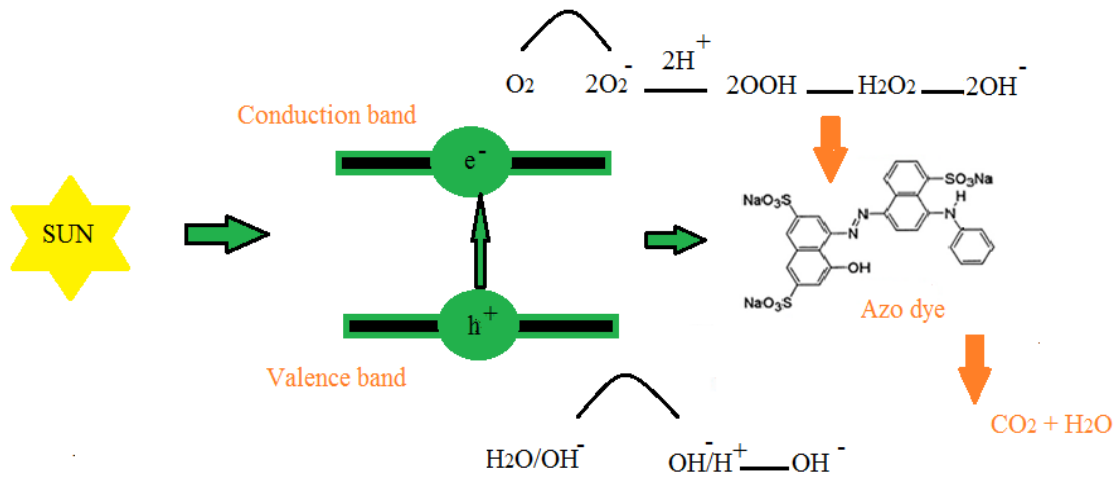


Fig. 10. Photo-catalyst mechanism in degradation of toxic dyes

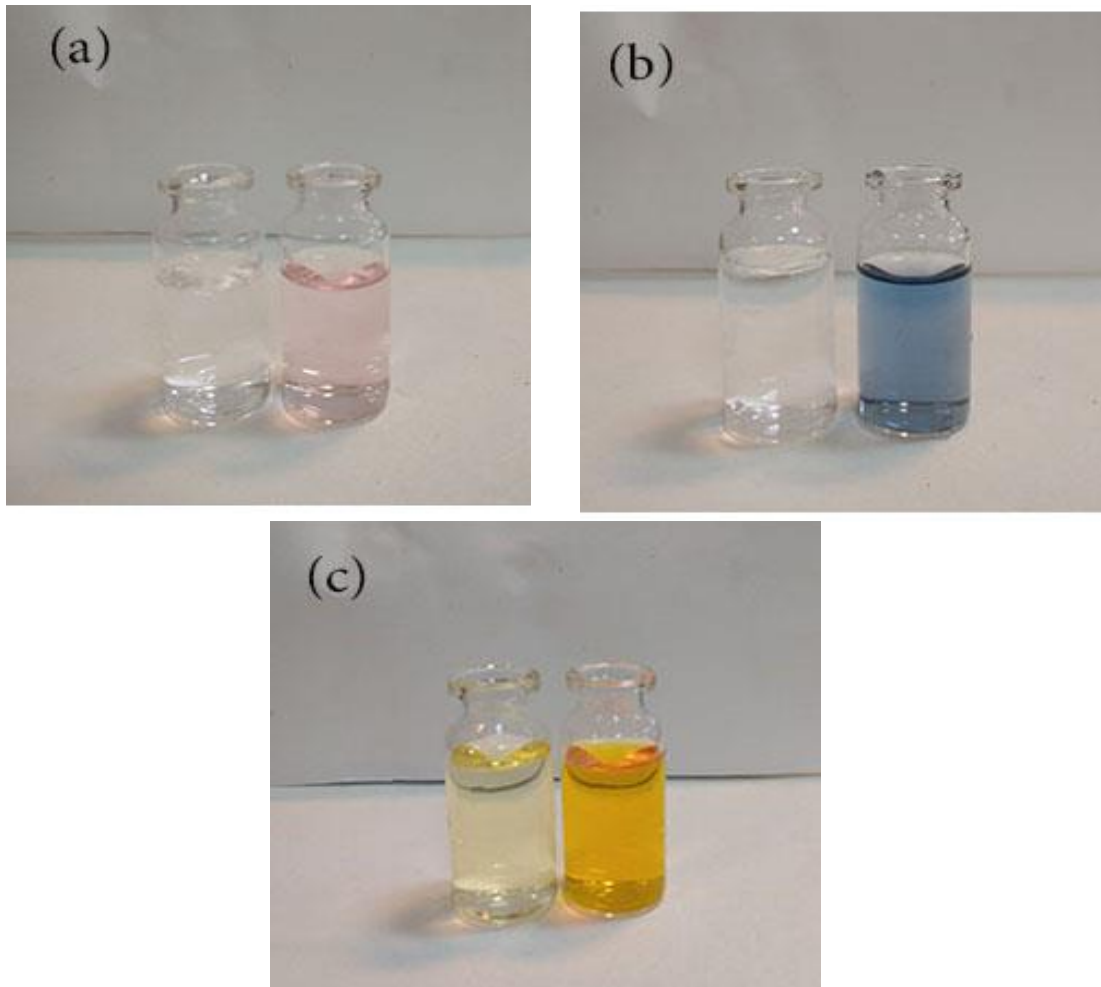


Fig. 11. Photo-degradation of Ag-doped (a) acid violet (b) acid blue (c) methyl orange

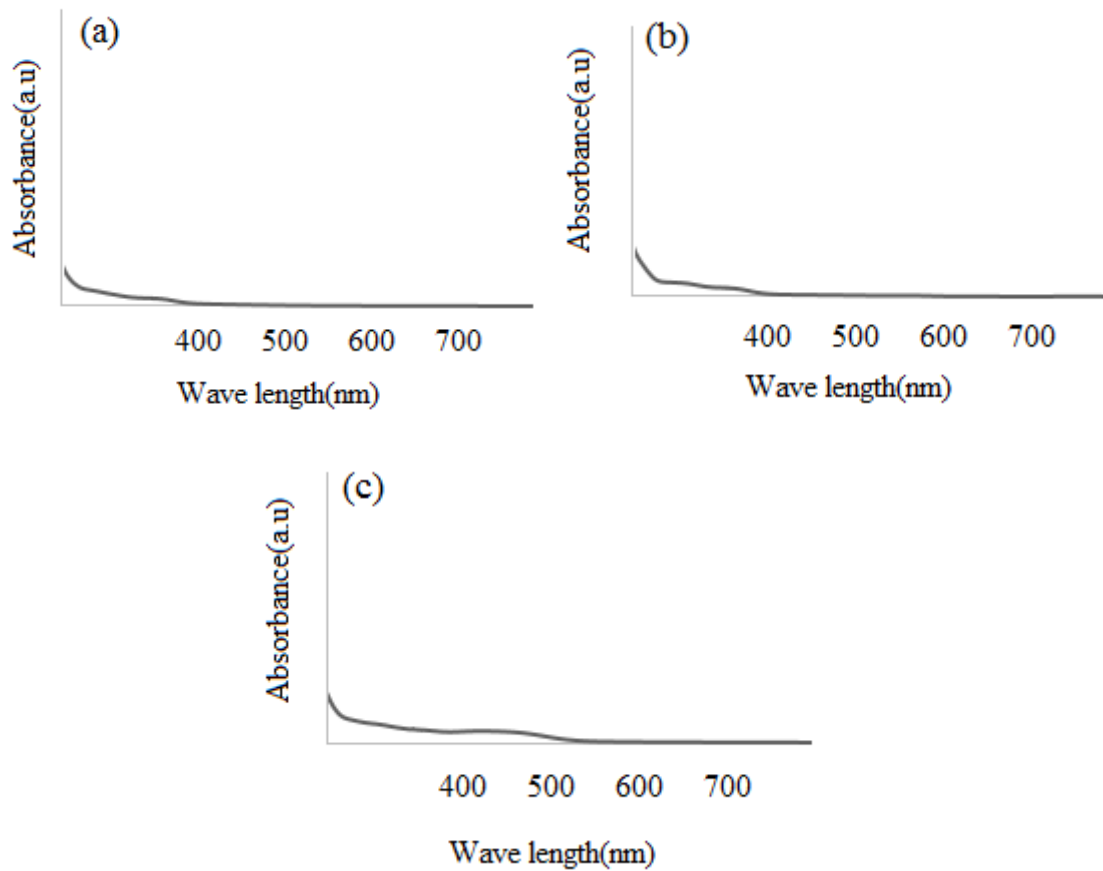


Fig. 12 UV-Visible absorption of dyes after irradiation a) (acid violet)b(acid blue)c(methyl orange

was evaluated by monitoring the degradation of organic dyes in an aqueous solution, under UV irradiation (Fig. 10). Acid violet, acid blue and methyl orange were degraded at 60 min respectively by CoFe_2O_4 -ZnS-Ag nanocomposite. As time increase, more and more dyes are adsorbed on the nanoparticles catalyst, until the absorption peaks (λ_{max}) of acid violet, acid blue and methyl orange decrease and vanish around 120 min (Fig. 11). The dyes concentration decreased rapidly with increasing UV-irradiation time organic dyes decompose to carbon dioxide, water and other less toxic or nontoxic residuals [25–26]. UV-visible spectro photometer was applied and it confirms in the presence of photo-catalyst under the UV-irradiation, the λ_{max} of all azo dyes were disappeared as it is shown in Fig. 12.

CONCLUSIONS

In conclusion, synthesis, characterization, and photocatalytic activity of CoFe_2O_4 , ZnS and

CoFe_2O_4 -ZnS-Ag nanocomposite were reported. AGFM confirmed that nanoparticles and nanocomposite exhibit either ferromagnetic or super-paramagnetic behaviour. The photocatalytic behaviour of CoFe_2O_4 -ZnS-Ag nanocomposite was evaluated using the degradation of three various azo dyes under UV light irradiation. The results show that precipitation method is a suitable method for preparation of CoFe_2O_4 -ZnS-Ag and other metal doped (Ni, Co, Cu) nanocomposites as a candidate for photocatalytic applications.

ACKNOWLEDGEMENTS

This work has been supported financially by Technical and Vocational University Lorestan Branch, under the Grant Number of 221/98/400/25.

CONFLICT OF INTEREST

The authors declare that there are no conflicts of interest regarding the publication of this

manuscript.

REFERENCES

- Harish S, Archana J, Navaneethan M, Ponnusamy S, Singh A, Gupta V, et al. Synergetic effect of CuS@ZnS nanostructures on photocatalytic degradation of organic pollutant under visible light irradiation. *RSC Advances*. 2017;7(55):34366-34375.
- Anjum M, Kumar R, Barakat MA. Visible light driven photocatalytic degradation of organic pollutants in wastewater and real sludge using ZnO-ZnS/Ag₂O-Ag₂S nanocomposite. *Journal of the Taiwan Institute of Chemical Engineers*. 2017;77:227-235.
- Sacco O, Vaiano V, Sannino D, Picca RA, Cioffi N. Ag modified ZnS for photocatalytic water pollutants degradation: Influence of metal loading and preparation method. *Journal of Colloid and Interface Science*. 2019;537:671-681.
- Fernández A, Lassaletta G, Jiménez VM, Justo A, González-Elipe AR, Herrmann JM, et al. Preparation and characterization of TiO₂ photocatalysts supported on various rigid supports (glass, quartz and stainless steel). Comparative studies of photocatalytic activity in water purification. *Applied Catalysis B: Environmental*. 1995;7(1-2):49-63.
- Lee G-J, Wu JJ. Recent developments in ZnS photocatalysts from synthesis to photocatalytic applications — A review. *Powder Technol*. 2017;318:8-22.
- Hao D, Zhang X, Ying W, Li T. Preparation of Zinc Sulfide Microspheres and Its Photocatalytic Activity on Antibiotics. *Asian J Chem*. 2013;25(4):1897-1900.
- Xu S, Han Y, Xu Y, Meng H, Xu J, Wu J, et al. Fabrication of polyaniline sensitized grey-TiO₂ nanocomposites and enhanced photocatalytic activity. *Sep Purif Technol*. 2017;184:248-256.
- Tobaldi DM, Pullar RC, Gualtieri AF, Seabra MP, Labrincha JA. Sol-gel synthesis, characterisation and photocatalytic activity of pure, W-, Ag- and W/Ag co-doped TiO₂ nanopowders. *Chem Eng J*. 2013;214:364-375.
- Sun J-X, Yuan Y-P, Qiu L-G, Jiang X, Xie A-J, Shen Y-H, et al. Fabrication of composite photocatalyst g-C₃N₄-ZnO and enhancement of photocatalytic activity under visible light. *Dalton Transactions*. 2012;41(22):6756.
- Chen F, Cao Y, Jia D, Niu X. Facile synthesis of CdS nanoparticles photocatalyst with high performance. *Ceram Int*. 2013;39(2):1511-1517.
- Ye Z, Kong L, Chen F, Chen Z, Lin Y, Liu C. A comparative study of photocatalytic activity of ZnS photocatalyst for degradation of various dyes. *Optik*. 2018;164:345-354.
- Pouretedal HR, Norozi A, Keshavarz MH, Semnani A. Nanoparticles of zinc sulfide doped with manganese, nickel and copper as nanophotocatalyst in the degradation of organic dyes. *J Hazard Mater*. 2009;162(2-3):674-681.
- Zhang Z, Xiao A, Yan K, Liu Y, Yan Z, Chen J. CuInS₂/ZnS/TGA Nanocomposite Photocatalysts: Synthesis, Characterization and Photocatalytic Activity. *Catal Lett*. 2017;147(7):1631-1639.
- Mohamed SH. Photocatalytic, optical and electrical properties of copper-doped zinc sulfide thin films. *J Phys D: Appl Phys*. 2010;43(3):035406.
- Lu M-Y, Lu M-P, Chung Y-A, Chen M-J, Wang ZL, Chen L-J. Intercrossed Sheet-Like Ga-Doped ZnS Nanostructures with Superb Photocatalytic Activity and Photoresponse. *The Journal of Physical Chemistry C*. 2009;113(29):12878-12882.
- Rao BP, Caltun O, Cho WS, Kim C-O, Kim C. Synthesis and characterization of mixed ferrite nanoparticles. *J Magn Magn Mater*. 2007;310(2):e812-e814.
- Caltun O, Rao GSN, Rao KH, Parvatheeswara Rao B, Dumitru I, Kim C-O, et al. The influence of Mn doping level on magnetostriction coefficient of cobalt ferrite. *J Magn Magn Mater*. 2007;316(2):e618-e620.
- Pan S, Liu X. ZnS-Graphene nanocomposite: Synthesis, characterization and optical properties. *J Solid State Chem*. 2012;191:51-56.
- Senapati KK, Borgohain C, Phukan P. CoFe₂O₄-ZnS nanocomposite: a magnetically recyclable photocatalyst. *Catalysis Science & Technology*. 2012;2(11):2361.
- Graphene Quantum Dots-ZnS Nanocomposites with Improved Photoelectric Performances. *Materials*. 2018;11(4):512.
- Asadi J, Golshan Ebrahimi N, Razzaghi-Kashani M. Self-healing property of epoxy/nanoclay nanocomposite using poly(ethylene-co-methacrylic acid) agent. *Composites Part A: Applied Science and Manufacturing*. 2015;68:56-61.
- Song E-H, Kang B-H, Kim T-Y, Lee H-J, Park Y-W, Kim Y-C, et al. Highly Oriented Gold/Nanoclay-Polymer Nanocomposites for Flexible Gas Barrier Films. *ACS Applied Materials & Interfaces*. 2015;7(8):4778-4783.
- Land G, Stephan D. Controlling cement hydration with nanoparticles. *Cem Concr Compos*. 2015;57:64-67.
- Lai CY, Groth A, Gray S, Duke M. Preparation and characterization of poly(vinylidene fluoride)/nanoclay nanocomposite flat sheet membranes for abrasion resistance. *Water Res*. 2014;57:56-66.
- Ali Dadfar SM, Alemzadeh I, Reza Dadfar SM, Vosoughi M. Studies on the oxygen barrier and mechanical properties of low density polyethylene/organoclay nanocomposite films in the presence of ethylene vinyl acetate copolymer as a new type of compatibilizer. *Materials & Design*. 2011;32(4):1806-1813.
- Ghanbari D, Sharifi S, Naraghi A, Nabiyouni G. Photo-degradation of azo-dyes by applicable magnetic zeolite Y-Silver-CoFe₂O₄ nanocomposites. *Journal of Materials Science: Materials in Electronics*. 2016;27(5):5315-5323.
- Shabani A, Nabiyouni G, Saffari J, Ghanbari D. Photocatalyst Fe₃O₄/TiO₂ nanocomposites: green synthesis and investigation of magnetic nanoparticles coated on cotton. *Journal of Materials Science: Materials in Electronics*. 2016;27(8):8661-8669.
- Ahmadian-Fard-Fini S, Salavati-Niasari M, Ghanbari D. Hydrothermal green synthesis of magnetic Fe₃O₄-carbon dots by lemon and grape fruit extracts and as a photoluminescence sensor for detecting of E. coli bacteria. *Spectrochimica Acta Part A: Molecular and Biomolecular Spectroscopy*. 2018;203:481-493.
- Ahmadian-Fard-Fini S, Ghanbari D, Amiri O, Salavati-Niasari M. Electro-spinning of cellulose acetate nanofibers/Fe/carbon dot as photoluminescence sensor for mercury (II) and lead (II) ions. *Carbohydr Polym*. 2020;229:115428.
- Moradi B, Nabiyouni G, Ghanbari D. Rapid photo-degradation of toxic dye pollutants: green synthesis of mono-disperse Fe₃O₄-CeO₂ nanocomposites in the presence of lemon extract. *Journal of Materials Science: Materials in Electronics*. 2018;29(13):11065-11080.
- Etmnan M, Nabiyouni G, Ghanbari D. Preparation of tin

ferrite-tin oxide by hydrothermal, precipitation and auto-combustion: photo-catalyst and magnetic nanocomposites for degradation of toxic azo-dyes. *Journal of Materials Science: Materials in Electronics*. 2017;29(3):1766-1776.

32. Ahmadian-Fard-Fini S, Ghanbari D, Salavati-Niasari M.

Photoluminescence carbon dot as a sensor for detecting of *Pseudomonas aeruginosa* bacteria: Hydrothermal synthesis of magnetic hollow NiFe₂O₄-carbon dots nanocomposite material. *Composites Part B: Engineering*. 2019;161:564-577.